Inorg. Chem. **2003**, *42*, 5871–5879

Synthesis and Spectroscopic and Structural Characterization of Two Novel Photoactivatable Ca^{2+} Compounds

Alessia Bacchi,[†] Mauro Carcelli,[†] Corrado Pelizzi,[†] Giancarlo Pelizzi,[†] Paolo Pelagatti,[†] Dominga Rogolino,*[,†,‡] Matteo Tegoni,[†] and Cristiano Viappiani[‡,§]

Dipartimento di Chimica Generale ed Inorganica, Chimica Analitica, Chimica Fisica, Università degli Studi di Parma, Parco Area delle Scienze 17/A, 43100 Parma, Italy, Dipartimento di Fisica, Università degli Studi di Parma, Parco Area delle Scienze 7/A, 43100 Parma, Italy, and INFM (Istituto Nazionale per la Fisica della Materia), Parma, Italy

Received January 20, 2003

Two novel photoactivatable Ca^{2+} compounds were synthesized to achieve a fast concentration jump of calcium ions in solution; this is of paramount importance for investigating the physiological cellular response. The light-sensitive ligands 4-(2-nitrophenyl)-3,6-dioxaoctane dioic acid (**H_2L^1**) and 4-(4,5-dimethoxy-2-nitrophenyl)-3,6-dioxaoctane dioic acid (**H_2L^2**) were generated by multistep syntheses, and the corresponding calcium complexes, **Ca(1)** and **Ca(2)**, were isolated and characterized. The solution equilibria of **H_2L^1** and **H_2L^2** with Ca^{2+} were investigated; for both ligands, the formation of a 1:2 Ca^{2+}/ligand species is detected and the complete characterization is presented. The crystal structures of **Ca(1)** and **Ca(2)** were determined. In **Ca(1)** the solid state assembly is attained by a polymeric association of [**($CaL^1(H_2O))_2(\mu$-OH_2)**] dimeric units. Each calcium ion coordinates four oxygen atoms of one ligand (two ethereal, one carboxylic, and one bridging carboxylic oxygen atom), one water molecule, one bridging water molecule, and a carboxylate group of the other ligand within the dimer. The octacoordination of the metal is completed by an interaction with the adjacent dimeric unit. The crystal structure of the complex **Ca(2)** does not show a polymeric nature, but it is a centrosymmetric dimer. The coordination number of the metal ion is still 8: 4 oxygen atoms of the ligand; 3 water molecules; 1 bridging carboxylate group. A preliminary study of the photochemical features of the complexes **Ca(1)** and **Ca(2)** is reported: photoexcitation by a nanosecond pulsed UV laser induces the cleavage of the ligand. This drastically reduces the affinity of the ligand toward Ca^{2+}, which is then released in solution.

Introduction

Calcium plays a key role in many biological and biochemical processes. Studies on calcium binding and release are critical to the meaningful interpretation of the biological functions and biochemical reactions with Ca^{2+} dependence. A rapid, selective concentration jump of calcium ion in solution is therefore highly desirable.[1−3] Recently, great interest has been turned on the so-called "*caged* compounds", molecules that are able to release biologically active species upon illumination.[4] The rationale for using caged compounds, and the reason for the continuous interest in developing new and improved caged analogues of biologically active molecules, is to exploit the temporal and spatial resolution afforded by using light to effect a change in concentration of the molecule of interest. The photocleavage reaction, in fact, generates the active biomolecule within a few milliseconds or faster and represents a major advanced in kinetic studies of cell function.[5−7]

Two alternative approaches for a rapid photogenerated increase in calcium concentration have been proposed, both

* To whom correspondence should be addressed. E-mail: dominga.rogolino@unipr.it.
† Dipartimento di Chimica Generale ed Inorganica, Chimica Analitica, Chimica Fisica, Università degli Studi di Parma.
‡ INFM.
§ Dipartimento di Fisica, Università degli Studi di Parma.

(1) Kaplan, J. H. *Annu. Rev. Physiol. Sci.* **1990**, *52*, 897−914.
(2) Adams, S. R.; Tsien, R. Y. *Annu. Rev. Physiol. Sci.* **1993**, *55*, 755−784.
(3) Giovannardi, S.; Landò, L.; Peres, A. *News Physiol. Sci*. **1998**, *13*, 251−255.
(4) Mariott, G. *Caged Compounds. Methods in Enzymology*; Academic Press: New York, London, 1998; Vol. 291.
(5) McCray, J. A.; Trentham, D. R. *Annu. Rev. Biophys. Chem*. **1989**, *18*, 239−248.
(6) Cameron, J. F.; Frechet, J. *J. Am. Chem. Soc.* **1991**, *113*, 4303−4309.
(7) Theriot, J. A.; Mitchison, T. J. *Nature* **1991**, *352*, 126−128.

10.1021/ic034059t CCC: $25.00
Published on Web 08/27/2003

Chart 1. Chemical Structures of Caged Calcium Complexes

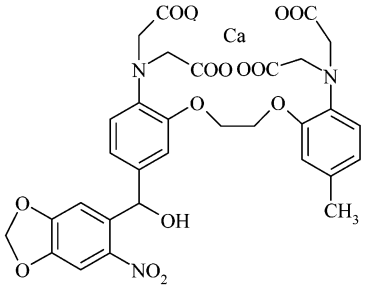

Nitr-5

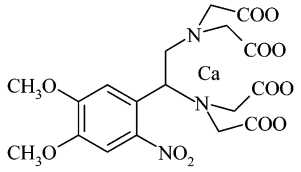

DM-nitrophen

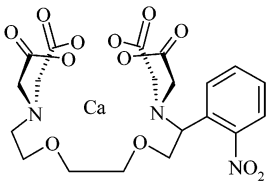

NP-EGTA

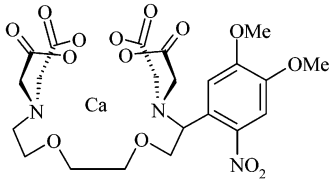

DMNPE-4

on the basis of the 2-nitrobenzyl chromophore, Nitr-5[8] and DM-nitrophen[9] (Chart 1). In the nitr series, the nitro group is reduced upon illumination and the alcoholic group is oxidated to a carbonyl; this decreases the electron-donating ability of the ligand and lowers the Ca^{2+} complex stability. On the contrary, irradiation of DM-nitrophen leads to the cleavage of the chelator and to the release of the calcium ion in solution.[10,11] Nitrophenyl-EGTA (NP-EGTA)[12] and DMNPE-4[13] (Chart 1), the most recent members of the family of nitrobenzyl ligands for calcium, work similarly to DM-nitrophen but have higher affinity for calcium over magnesium.

These Ca^{2+} complexes have found important applications in the context of cellular neurophysiology: they were used to study Ca^{2+} involvement in synaptic transmission, its effect on ion channel activity, and its role as second messenger for the activation in fibroblasts or in the regulation of muscle contraction.[2,14−15]

In this paper, we report the preparation of the light-sensitive ligands 4-(2-nitrophenyl)-3,6-dioxaoctane dioic acid (**H_2L^1**) and 4-(4,5-dimethoxy-2-nitrophenyl)-3,6-dioxaoctane dioic acid (**H_2L^2**) (Chart 2). In **H_2L^2**, the addition of methoxy substituents increases the λ_{max} of absorbance, which is of great importance for in vivo experiments, since it allows the use of light source at lower frequencies, avoiding protein photobleaching. Moreover, the two methoxy substituents are expected to increase the two-photon cross section of the 2-nitrobenzyl chromophore, making this compound a good candidate for two-photon uncaging.[16] The Ca^{2+} complexes of **H_2L^1** and **H_2L^2** (**Ca(1)** and **Ca(2)**, respectively) have been synthesized and characterized both in solution and in the solid state.

Chart 2. Chemical Structures of the Light-Sensitive Ligands **H_2L^1** and **H_2L^2**

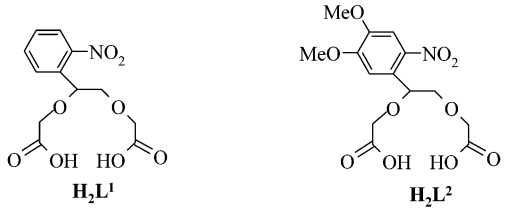

H_2L^1 **H_2L^2**

Scheme 1. Photolysis of the Light-Sensitive Complexes **Ca(1)** and **Ca(2)**[a]

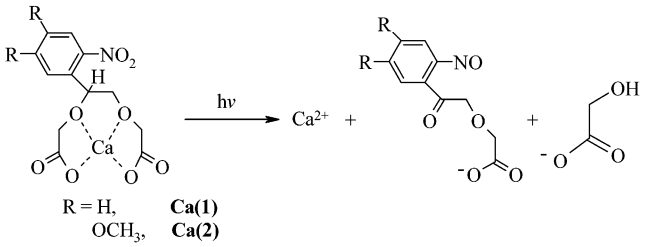

R = H, **Ca(1)**
OCH_3, **Ca(2)**

[a] Upon illumination, the ligand backbone is cleaved and the metal ion is released in solution.

It is expected[17] that, upon illumination, the reduction of the *o*-nitrobenzyl chromophore gives rise to the cleavage of the ligand backbone. The photoproducts show lower affinity to the metal ion, which is then rapidly released in solution (Scheme 1).

Experimental Section

Materials and Methods. Synthesis. All the reactions were carried out under nitrogen, by using standard Schlenk techniques; the solvents were dried according to literature methods and stored

(8) Adams, S. R.; Kao, J. P. Y.; Grynkiewicz, G.; Minta, A.; Tsien, R. Y. *J. Am. Chem. Soc.* **1988**, *110*, 3212−3220.
(9) Ellis-Davies, G. C. R.; Kaplan, J. H. *J. Org. Chem.* **1988**, *53*, 1966−1969.
(10) Kaplan, J. H.; Somlyo, A. P. *Trends Neurosci.* **1989**, *12*, 54−59.
(11) Kaplan, J. H. *Optical Methods in Cell Physiology*; Society for General Physiologists Series; DeWeer, P., Salzberg, B., Eds.; 1986; pp 417−446.
(12) Ellis-Davies, G. C. R.; Kaplan, J. H. *Proc. Natl. Acad. Sci. U.S.A.* **1994**, *91*, 187−191
(13) Ellis-Davies, G. C. R. *Tetrahedron Lett.* **1998**, *39*, 953−956.
(14) Nerbonne, J. M. *Curr. Opin. Neurobiol.* **1996**, *6*, 379−386.
(15) Park, M. K.; Tepikin, A. V. *Eur. J. Physiol.* **2002**, *444*, 305−316.
(16) Del Principe, F.; Egger, M.; Ellis-Davies, G. C. R.; Niggli, E. *Cell Calcium* **1999**, *25*, 85−91.
(17) Warmuth, R.; Grell, E.; Lehn, J.-M.; Bats, J. W.; Quinkert, G. *Helv. Chim. Acta* **1991**, *74*, 671−681.

over molecular sieves. All reagents of commercial quality were used without further purification.

Proton NMR spectra were recorded at 27 °C on a Bruker 300 FT spectrophotometer by using $SiMe_4$ as internal standard, while IR spectra were obtained with a Nicolet 5PCFT-IR spectrophotometer in the 4000−400 cm^{-1} range, using KBr disks. Elemental analyses were performed by using a Carlo Erba model EA 1108 apparatus.

The preparation of the ligands, $\mathbf{H_2L^1}$ and $\mathbf{H_2L^2}$, was made according to slightly modified literature methods.[17]

H_2L^1: ^{1}H NMR in $(CD_3)_2CO$ δ 8.02 (d, 1H, J = 8 Hz), 7.90 (d, 1H, J = 8 Hz), 7.80 (t, 1H, J = 8 Hz), 7.61 (t, 1H, J = 8 Hz), 5.41 (dd, 1H), 4.25−4.19 (m, 4H), 3.96−3.88 (m, 2H), 2.83 (s, broad, 1H, OH); IR (cm^{-1}) ν_{OH} = 3490, $\nu_{C=O}$ = 1727, 1687; MS-CI (pos ions) m/z 300 [MH^+, 20], 224 [M − CH_2COOH − OH, 100]. Anal. Calcd for $C_{12}H_{13}NO_8 \cdot 1.5H_2O$: C, 44.18; H, 4.94; N, 4.29. Found: C, 44.74; H, 5.15; N, 4.34.

H_2L^2: ^{1}H NMR in $(CD_3)_2SO$ δ 7.60 (s, 1H), 7.26 (s, 1H), 5.31 (dd, 1H), 4.12 (s, 2H), 4.00 (s, 2H), 3.89 (s, 3H), 3.86 (s, 3H), 3.72 (m, 2H), 3.25 (s, broad, 2H, OH); IR (cm^{-1}) ν_{OH} = 3425, $\nu_{C=O}$ = 1739, 1699; MS-CI (pos ions) m/z 359 [MH^+, 15], 284 [$(M - OCH_2COOH)^+$, 100]. Anal. Calcd for $C_{14}H_{17}NO_{10} \cdot H_2O$: C, 44.56; H, 5.07; N, 3.71. Found: C, 44.53; H, 4.99; N, 3.64.

$\{[(CaL^1(H_2O))_2(\mu\text{-}OH_2)] \cdot 0.4H_2O\}_n$, Ca(1). An aqueous solution of calcium hydroxide (49.5 mg, 0.66 mmol) was added dropwise to a methanolic solution (30 mL) of $\mathbf{H_2L^1}$ (200 mg, 0.66 mmol). The reaction mixture was stirred overnight at room temperature. After partial removal of the solvent, a white air stable solid was obtained, which was filtered off and washed with dichloromethane. Yield: 86%. Mp: 274−275 °C (dec). ^{1}H NMR in $(CD_3)_2SO$: δ 8.07 (d, 1H, J = 8 Hz), 7.85 (t, 1H, J = 7 Hz), 7.79 (d, 1H, J = 7 Hz), 7.64 (t, 1H, J = 8 Hz), 5.19 (dd, 1H, J = 7 Hz), 3.89 (dd, 1H, J = 10 Hz), 3.81−3.38 (m, 4 H). IR (cm^{-1}): ν_{OH} = 3420, $\nu_{C=O}$ = 1617. ESI-MS: m/z 338 [M^+, 100], 675 [$2M^+$, 25]. Anal. Calcd for $C_{12}H_{15}CaNO_{10}$: C, 38.61; H, 4.04; N, 3.74. Found: C, 38.82; H, 3.74; N, 3.74.

$[CaL^2(H_2O)_3]_2$, Ca(2). The synthesis was carried out as described for **Ca(1)**. The compound was obtained as a pale yellow powder. Yield: 62%. Mp: 251−252 °C (dec). ^{1}H NMR in D_2O: δ 7.88 (s, 1H), 7.38 (s, 1H), 5.64 (dd, 1H, J = 7 Hz), 4.65−3.96 (m, 6H), 4.08 (s, 3H), 4.04 (s, 3H). IR (cm^{-1}): ν_{OH} = 3406, $\nu_{C=O}$ = 1598. ESI-MS: m/z 397 [M^+, 100]. Anal. Calcd for $C_{14}H_{21}CaNO_{13}$: C, 37.25; H, 4.68; N, 3.10. Found: C, 37.66; H, 4.21; N, 3.15.

$Li_2Ca(L^1)_2 \cdot 2.5H_2O$, Ca(3). A 100 mg (0.33 mmol) amount of $\mathbf{H_2L^1}$ and 12 mg of lithium hydroxide (0.33 mmol) were dissolved in 30 mL of methanol. An aqueous solution of calcium hydroxide (0.165 mmol) was added dropwise over a period of 30 min. The reaction mixture was stirred overnight at room temperature. After partial removal of the solvent, a white solid, corresponding to **Ca(1)** (23 mg, 0.069 mmol), precipitates. It was filtered off, and from the filtrate, after complete removal of water, a white powder was isolated and characterized as **Ca(3)**. Yield: 40%. Mp: 167−168 °C (dec). ^{1}H NMR in D_2O: δ 8.16 (d, 2H, J = 8 Hz), 7.88 (m, 4H), 7.66 (t, 2H, J = 8 Hz), 5.41 (dd, 2H), 4.12 (s, 4H), 3.94−3.91 (m, 8H). IR (cm^{-1}): ν_{OH} = 3427, $\nu_{C=O}$ = 1609. ESI-MS: m/z: 648 [M^+, 25], 654 [$(M + Li)^+$, 100]. Anal. Calcd for $C_{24}H_{27}CaLi_2N_2O_{18.5}$: C, 41.57; H, 3.63; N, 4.03. Found: C, 41.80; H, 3.65; N, 4.07.

$Li_2Ca(L^2)_2 \cdot 6.5H_2O$, Ca(4). The synthesis was carried out as described for **Ca(3)**. The reaction mixture was stirred overnight at room temperature. After partial removal of the solvent, a white solid, corresponding to **Ca(2)** (20 mg, 0.052 mmol), precipitates. It was filtered off, and from the filtrate, after complete removal of water, a yellow powder was isolated and characterized as **Ca(4)**. Yield: 47%. Mp: 202−203 °C (dec). ^{1}H NMR in D_2O: δ 7.86 (s, 2H), 7.44 (s, 2H), 5.53 (dd, 2H), 4.07 (s, 6H), 4.03 (s, 6H), 4.12−3.85 (m, 12H). IR (cm^{-1}): ν_{OH} = 3422, $\nu_{C=O}$ = 1606. ESI-MS: m/z 768 [M^+, 30], 774 [$(M + Li)^+$, 100]. Anal. Calcd for $C_{28}H_{43}CaLi_2N_2O_{26.5}$: C, 37.98; H, 4.91; N, 3.13. Found: C, 37.74; H, 4.36; N, 3.03.

Potentiometric Measurements and Calculations. Methanolic solutions of the ligands (prepared by weight, ca. 0.02 mol dm^{-3}) were stocked at 4 °C and used within 3−4 days. Their titer was checked potentiometrically by titration with standard methanol/water (9:1, v/v) solutions of $(CH_3)_4NOH$ (Fluka, ca. 0.2 mol dm^{-3}). The concentration of $(CH_3)_4NOH$ solutions was determined potentiometrically by titration against potassium hydrogen phthalate (Merck, dried at 120 °C); the titer of the HCl solution (Merck Titrisol ampules, ca. 0.2 mol dm^{-3}) was derived by potentiometric titrations with $(CH_3)_4NOH$. Stock aqueous solution of $CaCl_2 \cdot 6H_2O$ and $MgCl_2 \cdot 6H_2O$ (Carlo Erba, ca. 0.02 mol dm^{-3}) were checked for concentration by complexometric titration with EDTA. All solutions were prepared with doubly distilled water and HPLC grade methanol, both freshly boiled. Titrations were carried out in methanol/water (9:1, v/v) mixtures at T = 25 ± 0.1 °C and I = 0.1 mol dm^{-3} ($(CH_3)_4NCl$), under N_2 atmosphere. The potentiometric apparatus for the automatic data acquisition (vol, E) was previously described.[18] An Hamilton glass combined electrode (P/N 238000) was modified according to literature methods,[19] filling the reference compartment with a 0.1 mol dm^{-3} $(CH_3)_4NCl$ methanol/water (9:1, v/v) solution. The electrodic chain was calibrated in terms of $[H^+]$ by titrating HCl solutions with methanol/water standard $(CH_3)_4NOH$ (pK_w = 14.43(1)). Acidity constants were determined by alkalimetric titration of three samples ((2−3) × 10^{-3} mol dm^{-3}). For the Ca^{2+} complexation equilibria, three to four titrations were carried out with Ca^{2+}/ligand molar ratios from 1:1 to 1:2.5, C_{Ca} ranging between 0.8 × 10^{-3} and 1.1 × 10^{-3} mol dm^{-3}. For the Mg^{2+} complexation equilibria, three to four titrations were carried out with Mg^{2+}/ligand molar ratios from 1:1 to 1:2.1, C_{Mg} ranging between 1.1 × 10^{-3} and 1.8 × 10^{-3} mol dm^{-3}.

Stability constants were calculated by the Hyperquad 2000 program.[20] The weighting of the experimental observations takes into account the errors of both emf and titrant volumes that were estimated as 0.2 mV and 0.008 cm^3, respectively.

X-ray Crystallography. Single crystals of **$Ca(2) \cdot 2H_2O$** and **Ca(1)** suitable for X-ray structure analysis were obtained by slow recrystallization from a methanol solution of the complexes. X-ray diffraction data were collected at room temperature on a Bruker-Siemens SMART AXS 1000 equipped with CCD detector, using graphite-monochromated Mo Kα radiation (λ = 0.710 73 Å). Data collection details are as follows: crystal to detector distance = 5.0 cm for **Ca(1)** and 4.0 cm for **$Ca(2) \cdot 2H_2O$**; 2424 frames collected (complete sphere mode); time per frame = 30 s; oscillation $\Delta\omega$ = 0.300°. Crystal decay was negligible in both cases. Data were processed by the SAINT package[21] and corrected for absorption effects by the SADABS[22] procedure (T_{max}/T_{min} = 1.000/0.851 for **Ca(1)** and 1.000/0.852 for **$Ca(2) \cdot 2H_2O$**). Data reduction was performed up to d = 0.80 Å for **Ca(1)**) and 0.90 Å for **Ca(2)·**

(18) Dallavalle, F.; Folesani, G.; Marchelli, R.; Galaverna, G. *Helv. Chim. Acta* **1994**, *77*, 1623−1630.
(19) Fisicaro, E.; Braibanti, A. *Talanta* **1988**, *35*, 769−774.
(20) Gans, P.; Sabatini, A.; Vacca, A. *Talanta* **1996**, *43*, 1739−1753.
(21) SAINT: *SAX, Area Detector Integration*; Siemens Analytical instruments Inc.: Madison, WI.
(22) SADABS: *Area-Detector Absorption Correction*; Siemens Industrial Automation, Inc.: Madison, WI, 1996.

Table 1. Crystal Data and Structure Refinement for **Ca(1)** and **Ca(2)·2H$_2$O**

param	**Ca(1)**	**Ca(2)**·2H$_2$O
empirical formula	$C_{24}H_{30}Ca_2N_2O_{20}$	$C_{14}H_{23}CaNO_{14}$
fw	746.66	469.41
cryst system	triclinic	monoclinic
space group	$P\bar{1}$	$P2_1/c$
unit cell dimens (Å, deg)	$a = 8.3513(9)$, $\alpha = 91.168(2)$ $b = 11.993(1)$, $\beta = 94.070(2)$ $c = 16.433(2)$, $\gamma = 105.891(2)$	$a = 14.0519(7)$ $b = 10.4258(5)$, $\beta = 103.961(1)$ $c = 14.3319(7)$
V (Å^3)	1577.6(3)	2037.6(2)
Z	2	4
D(calcd) (Mg/m^3)	1.572	1.530
abs coeff (mm^{-1})	0.452	0.381
F(000)	776	984
crystal size (mm^3)	0.4 × 0.6 × 0.6	0.3 × 0.5 × 0.9
θ range for data collcn (deg)	1.77−26.40	1.49−23.28
index ranges	$-10 \le h \le 9$, $-14 \le k \le 14$, $-20 \le l \le 20$	$-15 \le h \le 15$, $-11 \le k \le 11$, $-15 \le l \le 15$
rflcns collcd	9032	17 713
indpdt reflcns	6258 [R(int) = 0.0169]	2932 [R(int) = 0.0344]
data/restraints/params	6258/15/494	2932/8/362
goodness-of-fit on F^2	1.038	1.049
final R indices [$I > 2\sigma(I)$]	R1 = 0.0411, wR2 = 0.1143	R1 = 0.0379, wR2 = 0.0997
R indices (all data)	R1 = 0.0560, wR2 = 0.1234	R1 = 0.0507, wR2 = 0.1068

2H$_2$O. The phase problem was solved by direct methods[23] and refined by full-matrix least squares on all F^2.[24] Anisotropic displacement parameters were refined for all non-hydrogen atoms, while hydrogen atoms were located from difference Fourier maps for **Ca(2)·2H$_2$O** and for water molecules in **Ca(1)**; the remaining hydrogens were introduced in idealized positions. In **Ca(1)** a conformational disorder was found for the atoms O11−C21−C22−O13, which describe a planar chelation ring distributed on two differently populated (60:40) positions, with the O11−O12 vector as a fixed hinge. The solvation water molecule occupancy is related to the minor population. The discussion of structural results has been carried out by considering the major conformer. The final maps were featureless in both cases. Details of data collection and structure refinement are in Table 1. For the discussion use was made of the Cambridge Structural Database facilities.[25]

Absorption and Fluorescence Spectroscopy. The low affinity (K_d = 20 μM) free Ca^{2+} indicator Oregon Green 488 5N (OG5N) was from Molecular Probes (Eugene, OR). $CaCl_2$, $MgCl_2$, KCl, NaCl, and Hepes were from Sigma-Aldrich. Steady-state absorbance spectra were measured using a Jasco 7850 double beam, UV−visible spectrophotometer. Fluorescence emission was recorded by using a Perkin-Elmer LS50 steady-state spectrofluorometer. The laser flash photolysis set up was described previously.[26] Photolysis was achieved by means of the third harmonic of a nanosecond, Q-switched Nd:YAG laser (Surelite II-10, Continuum). The beam was passed through a variable attenuator (Eksma) and focused to a horizontal line with a 0.5 m cylindrical lens. The monitoring beam was a multiline, single-mode, CW Argon-ion laser (JDS Uniphase). The desired output line from the argon laser was selected using a Pellin Broca prism and an iris diaphragm. The quartz cuvette was held in a temperature-controlled (T = 20 °C) sample holder (FLASH 100, Quantum Northwest, Inc.). The monitoring beam was passed through a monochromator and detected by a preamplified (Avtech, AV149) avalanche silicon photodiode (Hamamatsu, S2382). The overall bandwidth exceeded 500 MHz. The voltage signal was digitized by a digital sampling oscilloscope (LeCroy 9370, 1 GHz, 1 GS/s). The sample (100 μL) was changed after each flash. To increase the signal-to-noise ratio, the pulse traces from 4 samples were averaged. To minimize bleaching of the OG5N samples by the intense monitoring laser beam, a fast mechanical shutter (Uniblitz) was opened only during data acquisition. The shutter driver provided a convenient synchronous output on shutter opening that was used to trigger a home-built delay line that fired the laser 100 ms later. Exposure times were never longer than 200 ms. The kinetics of the systems under investigation are extended in time, and therefore, the kinetic traces were recorded on different time scales to cover the complete time evolution. The traces were then merged to give a single, 50 000 points trace and eventually logarithmically down-sampled before analysis to 300 point data sets.

Results and Discussion

Synthesis and Characterization of the Complexes. The light-sensitive ligands **H$_2$L^1** and **H$_2$L^2** (Chart 2) were synthesized by following a strategy previously described.[17] The corresponding new calcium complexes, **Ca(1)** and **Ca(2)**, were obtained by adding dropwise an aqueous solution of $Ca(OH)_2$ to a methanolic solution of the free ligands. Attempts to obtain the calcium complexes by using $CaCO_3$ and $CaCl_2$ were unsuccessful. The anionic nature of the ligands is confirmed by the IR and the ^{1}H NMR spectra. In the IR spectrum, in fact, the C=O bands shift to lower frequencies (ν(C=O): **H$_2$L^1**, 1727, 1687 cm^{-1}; **Ca(1)**, 1617 cm^{-1}; **H$_2$L^2**, 1739, 1699 cm^{-1}; **Ca(2)**, 1598 cm^{-1}), while the signals relative to the carboxylic OH groups, both in the IR and ^{1}H NMR spectra, disappear. For both the complexes, crystals suitable for X-ray diffraction were obtained by slow evaporation of their methanolic solutions.

The determination of the equilibrium constants were carried out in methanol/water solutions (9:1, v/v) because of the poor solubility of the ligands in water (less than 10^{-3} M). To avoid the interference of alkaline metal ions such as K^+ or Na^+, $(CH_3)_4NCl$ was employed as background inert salt (I = 0.1 M). The acidity constants of the ligands **H$_2$L^1**

(23) Altomare, A.; Cascarano, G.; Giacovazzo, C.; Guagliardi, A.; Burla, M. C.; Polidori G.; Camalli, M. *J. Appl. Crystallogr.* **1994**, *27*, 435−442.
(24) SHELXL97, Sheldrick, G. M. *SHELXL97, Program for structure refinement*; University of Goettingen: Goettingen, Germany, 1997.
(25) Allen, F. H.; Kennard, O.; Taylor, R. *Acc. Chem. Res.* **1983**, *16*, 146−153.
(26) Abbruzzetti, S.; Viappiani, C.; Small, J. R.; Libertini, L. J.; Small, E. W. *J. Am. Chem. Soc.* **2001**, *123*, 6649−6653.

Table 2. Acidity Constants (pK_a) of $\mathbf{H_2L^1}$ and $\mathbf{H_2L^2}$ in Methanol/Water Mixture[a] (9:1, v/v). $T = 25$ °C, $I = 0.1$ mol dm^{-3} ($(CH_3)_4NCl$). Standard deviations are given in parentheses[a]

	H_2L^1	H_2L^2
pK_1	5.29(1)	5.27(1)
pK_2	6.17(1)	6.20(1)
σ^a	1.62	1.75
n^a	177	183

[a] $\sigma = [\Sigma w_i(E_i^o - E_i^c)^2/(n-m)]^{1/2}$ = sample standard deviation; $w_i = 1/\sigma_i^2$, where σ_i is the expected error on each experimental emf value (E_i^o); n = number of observations; m = number of parameters refined.

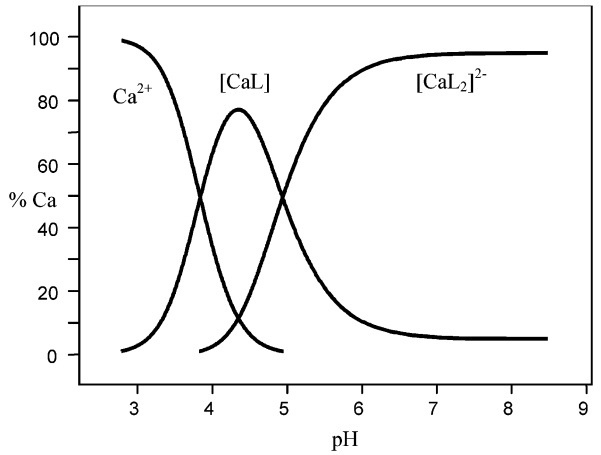

Figure 1. Distribution diagram of the system **Ca/$\mathbf{H_2L^1}$** ($Ca/H_2L^1 = 1:2.2$, $C_{Ca} = 1 \times 10^{-3}$ mol dm^{-3}).

Table 3. Ca^{2+} Complex Formation Constants (log β) of $\mathbf{H_2L^1}$ and $\mathbf{H_2L^2}$ in Methanol/Water Mixture (9:1, v/v). $T = 25$ °C, $I = 0.1$ mol dm^{-3} ($(CH_3)_4NCl$). Standard deviations are given in parentheses[a]

	$[CaL^1]$	$[CaL^1_2]^{2-}$	$[CaL^2]$	$[CaL^2_2]^{2-}$
log β	6.59(1)	11.52(1)	6.55(1)	11.52(1)
σ_a	2.45	2.45	2.35	2.35
n^a	210	210	215	215

[a] See Table 2.

and $\mathbf{H_2L^2}$ are very similar (see Table 2). Their values are higher than those determined for the ligand 1,2-bis(carboxymethoxy)ethane in water solution ($pK_{a1} = 2.99$, $pK_{a2} = 3.83$),[27] and this is mainly due to the different solvents employed. In fact the pK_a of a neutral acid, such as a carboxylic acid, usually increases remarkably from pure water to a methanol/water mixture.[28] The speciation models for the Ca^{2+} complexes with the ligands $\mathbf{H_2L^1}$ and $\mathbf{H_2L^2}$ consist of **CaL** and $\mathbf{[CaL_2]^{2-}}$ ($\mathbf{H_2L} = \mathbf{H_2L^1}$, $\mathbf{H_2L^2}$) (Figure 1); the complex formation constants are practically identical (see Table 3). As in the solid state the complex **Ca(2)** has a dimeric nature (see below); the formation of the $\mathbf{Ca_2L^2_2}$ species was taken into account in the refinement of the formation constants, giving a worse fitting, and then rejected.

The **CaL** log β values were obtained also from fluorescence data in water (log β(**Ca(1)**) = 5.6(4); log β(**Ca(2)**) = 5.7(3)). The two different sets of log β values are well compatible if the solvent effect, which makes the formation of the less solvated neutral complexes **CaL** more favorable in methanol than in water, is considered.

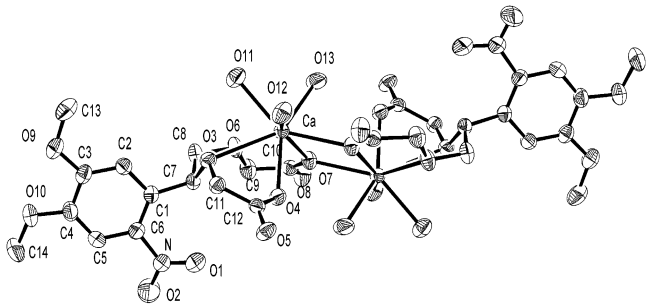

Figure 2. Molecular structure of **Ca(2)** as determined by X-ray diffraction. The dimer is centrosymmetric. Hydrogens and solvation waters are omitted for clarity.

Table 4. Most Relevant Bond Distances (Å) and Angles (deg) for **Ca(2)·2H_2O**, with Su's in Parentheses[a]

Ca−O12	2.347(2)	Ca−O11	2.422(2)
Ca−O13	2.373(2)	Ca−O6	2.466(2)
Ca−O4	2.397(2)	Ca−O7(i)	2.510(2)
Ca−O7	2.414(2)	Ca−O3	2.821(2)
O12−Ca−O13	103.0(1)	O11−Ca−O6	74.79(8)
O12−Ca−O4	84.61(8)	O12−Ca−O7(i)	80.27(7)
O13−Ca−O4	150.56(8)	O13−Ca−O7(i)	76.27(8)
O12−Ca−O7	152.37(8)	O4−Ca−O7(i)	77.12(7)
O13−Ca−O7	75.99(8)	O7−Ca−O7(i)	72.62(7)
O4−Ca−O7	84.26(7)	O11−Ca−O7(i)	141.08(8)
O12−Ca−O11	79.79(8)	O6−Ca−O7(i)	137.84(7)
O13−Ca−O11	76.14(8)	O12−Ca−O3	77.99(7)
O4−Ca−O11	133.27(7)	O13−Ca−O3	148.15(8)
O7−Ca−O11	125.38(8)	O4−Ca−O3	61.01(6)
O12−Ca−O6	138.87(8)	O7−Ca−O3	117.65(6)
O13−Ca−O6	101.63(9)	O11−Ca−O3	72.71(7)
O4−Ca−O6	89.80(7)	O6−Ca−O3	63.91(6)
O7−Ca−O6	66.24(6)	O7(i)−Ca−O3	134.07(6)

[a] Symmetry transformations used to generate equivalent atoms: (i) $-x$, $-y$, $-z + 2$.

Although there are some papers dealing with the Ca^{2+} complexation with the ligand 1,2-bis(carboxymethoxy)ethane,[27,29] the formation of the species $\mathbf{[CaL_2]^{2-}}$ was never reported previously. To confirm the model, the complexes **Ca(3)** and **Ca(4)** were synthesized by using a Ca^{2+}:L = 1:2 molar ratio (see Experimental Section).

Magnesium ions, which are normally present in cellular medium, can interfere with caged calcium complexes. Therefore, the log β values for the **MgL** species were also determined ($\mathbf{MgL^1}$ log $\beta = 4.14(1)$; $\mathbf{MgL^2}$ log $\beta = 4.15(1)$). These complexes are less stable than the corresponding calcium ones (ca. 2.4 log units); no $\mathbf{[MgL_2]^{2-}}$ species were found.

X-ray Crystallography. Compound **Ca(2)** crystallizes as a dihydrate with formula $\mathbf{[CaL^2(H_2O)_3]_2 \cdot 2H_2O}$. The molecular structure of **Ca(2)** is shown in Figure 2, while the most relevant geometric parameters are in Table 4.

The complex consists of a centrosymmetric heterochiral dimer, where two equivalent calcium ions are coordinated to two bideprotonated ligands related by the symmetry operation i = $-x$, $-y$, $2 - z$. Each metal is chelated by the O_4 donor system formed by the two ethereal and two

(27) Miyiazaki, M.; Shimoishi, Y.; Miyata, H.; Tôei, K. *J. Inorg. Nucl. Chem.* **1974**, *36*, 2033−2038.
(28) Rorabacher, D. B.; MacKellar, W. J.; Shu, F. R.; Bonavita, M. *Anal. Chem.* **1971**, *43*, 561−573.
(29) Ancillotti, F.; Boschi, G.; Perego, G.; Zazzetta, A. *J. Chem. Soc., Dalton Trans.* **1977**, *901*, 1972−1999.

Table 5. List of Hydrogen Bonds in the Crystal Structure of **Ca(2)·2H$_2$O**

	D···A (Å)	D−H···A (deg)
O13−H···O14	2.790(4)	166 (3)
O12−H···O5(1)	2.732(3)	172(2)
O11−H···O5(2)	2.749(3)	163(2)
O11−H···O14(3)	2.855(4)	155(4)
O14−H···O8(4)	2.830(5)	166(3)
O12−H···O8(5)	2.686(3)	161(3)
O13−H···O4(5)	2.789(3)	169(3)
equiv posns	(1) $-x, y + 1/2, -z + 3/2$	(3) $-x, -y + 1, -z + 2$
	(2) $x, -y + 1/2, z + 1/2$	(4) $-x, y + 1/2, -z + 5/2$
		(5) $-x, -y, -z + 2$

carboxylic oxygens (O3, O6, O4, and O7, respectively) and is additionally coordinated to a second carboxylic oxygen belonging to the second ligand (O7(i)). The metal achieves the octacoordination by binding three water molecules. The two flexible ligand arms are folded to embrace the cation; the arm conformations are described by the torsion angles C1−C7−C8−O6 = −171.8(2)° and C7−C8−O6−C9 = 99.5(3)° for the longest arm and C1−C7−O3−C11 = 73.8(3)° for the shortest one. The binding system of both the two asymmetric ligand arms are based on two $-O-CH_2-C(O)O^-$ planar systems which chelate the metal defining two five-membered chelation rings O−C−C−O−Ca. The two chelation systems are tilted and form a dihedral angle of 58°. Nevertheless, the four oxygens of the O_4 donor set are coplanar within 0.2 Å, defining an approximately square cavity with edges in the range 2.7−3.2 Å. The calcium atom is remarkably displaced out of the O_4 average plane by 1.5 Å. The remaining four donors O11, O12, O13, and O7(i) also form an approximately square system, with edges ranging between 2.9 and 3.1 Å (maximum deviation from planarity = 0.35 Å), and the metal atom is displaced by 1.1 Å from this second O_4 square. The two planes defined by the two donor sets are almost parallel (dihedral angle = 7°), giving rise to an irregular square antiprism, with average tilt angle close to 45°.

The Ca−O distances are remarkably variable, the shortest ones involving water molecules, and the longest ones regarding ethereal donors. In particular, the bond to the oxygen directly bonded to the chiral carbon is very weak (Ca−O3 = 2.821(2) Å), significantly longer than the sum of covalent radii (2.47 Å).

The two coordination polyhedra in the complex dimer share the oblique O7−O7(i) edge, while the O_4 squares are all almost coplanar; the Ca···Ca(i) distance in the dimer is 3.97 Å.

The aromatic substituent is almost perpendicular to the ligand coordination plane (dihedral angle = 80°); the nitro group is practically coplanar to the aromatic ring (O1−N−C6−C1 = 23.2(5)°) and points toward the CH group on the chiral carbon C7, forming the intramolecular hydrogen bond C7−H···O1 (C7···O1 = 2.811(5) Å, H···O1 = 2.12(3) Å, C7−H···O1 = 126(2)°).

The structure is characterized by an extensive network of hydrogen bonds involving also the solvation water, as reported in Table 5.

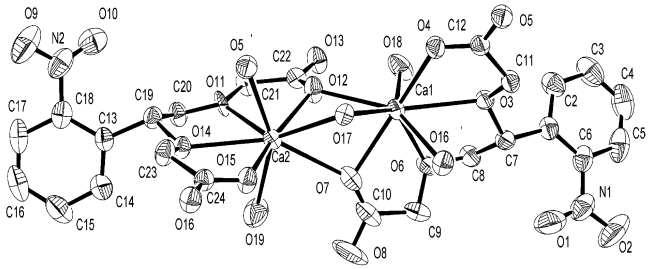

Figure 3. Asymmetric unit for **Ca(1)**, showing the dimeric unit. The octacoordination of each metal is completed by a bridging interaction towards adjacent units, involving O5 and O16. The flattening of the ligand compared to Figure 2 is evident. Hydrogens, disordered portions and uncoordinated water are omitted for clarity.

Table 6. Most Relevant Bond Distances (Å) and Angles (deg) for **Ca(1)**, with Su's in Parentheses

Ca1−O4	2.359(2)	Ca2−O15	2.333(1)
Ca1−O18	2.371(2)	Ca2−O12	2.390(2)
Ca1−O7	2.382(2)	Ca2−O17	2.398(2)
Ca1−O17	2.417(1)	Ca2−O19	2.404(2)
Ca1−O6	2.431(2)	Ca2−O11	2.41(2)
Ca1−O16(i)	2.505(2)	Ca2−O5(ii)	2.444(2)
Ca1−O12	2.537(2)	Ca2−O14	2.566(2)
Ca1−O3	2.620(1)	Ca2−O7	2.717(2)
O4−Ca1−O18	89.35(7)	O15−Ca2−O12	161.96(6)
O4−Ca1−O7	155.47(7)	O15−Ca2−O17	89.22(6)
O18−Ca1−O7	114.23(7)	O12−Ca2−O17	73.16(6)
O4−Ca1−O17	85.99(6)	O15−Ca2−O19	82.66(9)
O18−Ca1−O17	138.29(7)	O12−Ca2−O19	111.04(9)
O7−Ca1−O17	72.01(6)	O17−Ca2−O19	128.04(7)
O4−Ca1−O6	129.21(6)	O15−Ca2−O11	125.6(3)
O18−Ca1−O6	78.71(7)	O12−Ca2−O11	68.3(3)
O7−Ca1−O6	65.74(6)	O17−Ca2−O11	134.8(4)
O17−Ca1−O6	133.62(6)	O19−Ca2−O11	88.3(6)
O4−Ca1−O16(i)	84.59(6)	O15−Ca2−O5(ii)	83.96(6)
O18−Ca1−O16(i)	143.29(7)	O12−Ca2−O5(ii)	88.17(7)
O7−Ca1−O16(i)	80.21(6)	O17−Ca2−O5(ii)	76.75(5)
O17−Ca1−O16(i)	77.43(5)	O19−Ca2−O5(ii)	151.43(7)
O6−Ca1−O16(i)	77.43(6)	O11−Ca2−O5(ii)	79.2(6)
O4−Ca1−O12	113.16(6)	O15−Ca2−O14	64.33(5)
O18−Ca1−O12	73.73(7)	O12−Ca2−O14	128.77(5)
O7−Ca1−O12	70.06(6)	O17−Ca2−O14	142.37(5)
O17−Ca1−O12	70.29(5)	O19−Ca2−O14	77.09(7)
O6−Ca1−O12	110.32(6)	O11−Ca2−O14	61.3(3)
O16(i)−Ca1−O12	141.29(5)	O5(ii)−Ca2−O14	74.37(5)
O4−Ca1−O3	63.52(5)	O15−Ca2−O7	110.09(6)
O18−Ca1−O3	74.40(6)	O12−Ca2−O7	66.86(6)
O7−Ca1−O3	127.32(6)	O17−Ca2−O7	66.61(5)
O17−Ca1−O3	136.98(5)	O19−Ca2−O7	68.51(7)
O6−Ca1−O3	65.72(5)	O11−Ca2−O7	115.9(4)
O16(i)−Ca1−O3	70.51(5)	O5(ii)−Ca2−O7	140.03(6)
O12−Ca1−O3	147.99(5)	O14−Ca2−O7	145.60(5)

[a] Symmetry transformations used to generate equivalent atoms: (i) $-x + 2, -y, -z + 1$; (ii) $-x + 1, -y, -z + 1$.

The relevant role of hydration level on the structural organization of the calcium complex becomes evident when we analyze the **Ca(1)** solid state arrangement, in which dimeric units further condensate in a polymeric structure. The solid-state structure of **Ca(1)** is based on the dimeric homochiral unit shown in Figure 3, where the two monomeric octacoordinated complexes are symmetry independent, but with similar coordination arrangements. Both the dimeric enantiomers are present in the centrosymmetric crystal, giving a racemic solid. The relevant bonding features are listed in Table 6.

Both independent ligands coordinate the two calcium ions by the O_4 donor set formed by the two ethereal (O3, O6 and

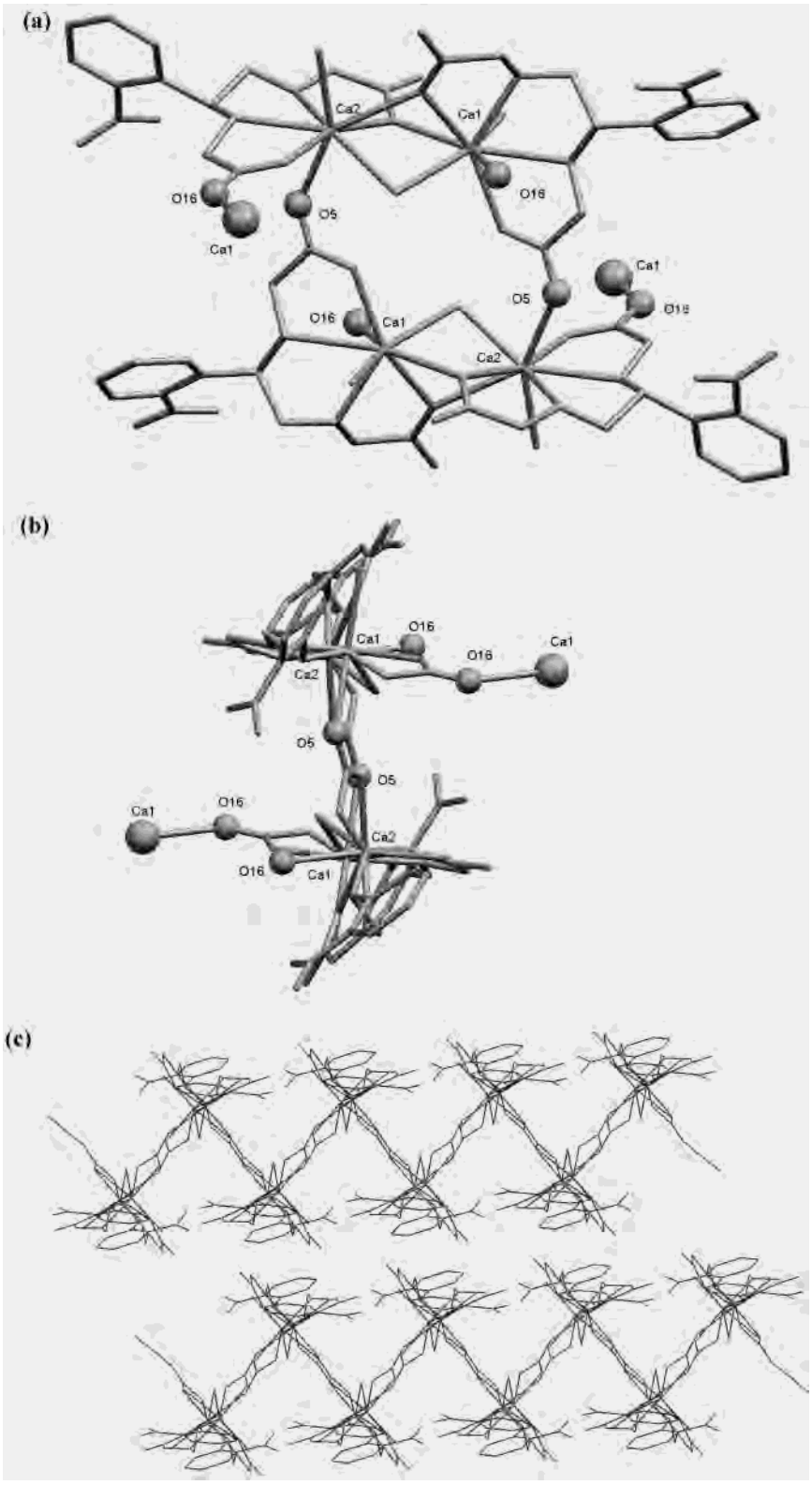

Figure 4. (a) Association of dimers in centrosymmetric tetramers for **Ca(1)** as a starting point for the polymeric chain formation. The expansion of the polymer is achieved through the bridging interactions O5−Ca2 and O16−Ca1 (evidenced). (b) Side view of the tetrameric unit shown in (a), illustrating that the bridging interactions take place in perpendicular planes. (c) Polymeric chains in **Ca(1)**.

O11, O14 for the two molecules) and the two carboxylic oxygens (O4, O7 and O12, O15). The coordination sphere of each metal is then filled with two water molecules, one of which, O17, is shared by the two ions in a bridged fashion. The octacoordination of each cation is completed by coordinating the carboxylic oxygen already bonded to the other metal (O7 and O12) and one carboxylic oxygen belonging to adjacent complex dimeric units of opposite chirality (Ca1−O16 ($-x + 2$, $-y$, $-z + 1$), Ca2−O5 ($-x + 1$, $-y$, $-z + 1$)). The stoichiometry of the polymer is

then $\{[Ca(L^1)(H_2O)]_2(\mu\text{-}H_2O)\}_n$. One disordered, partially occupied (40%), crystallization water/dimeric unit completes the crystal structure. The packing of the dimers in a more compact polymeric structure, and the consequent bridging role played by one coordinated water and by the carboxylates produces a conformational modification on the ligand and a deformation of the coordination geometry with respect to **Ca(2)**. The O_4 donor sets are both planar within 0.23 Å. For both ligands the calcium atom is roughly contained in the plane defined by the O_4 donor set (deviations of 0.36 and 0.03 Å for Ca1 and Ca2, respectively), while the chelation systems defining the O_4 donor set are still tilted but to different extents in the two molecules (dihedral angles of 69 and 23° between the $-O-CH_2-C(O)O^-$ planes in the two independent ligands). In **Ca(1)** the ligand is considerably flattened if compared with **Ca(2)**. The entrance of the cation in the core of the ligand embrace produces a different folding of the ligand arms compared to the previously described **Ca(2)** compound (**Ca(1)**: C1−C7−C8−O6 = −176.6(2)°, C7−C8−O6−C9 = −96.9(2)°, C1−C7−O3−C11 = −71.7(2)°, C13−C19−C20−O11 = −169(1)°, C19−C20−O11−C21 = −159(1)°, C13−C19−O14−C23 = −67.1(2)°); consequently, the external O···O edges of the polygon defined by the O_4 donor sets are elongated with respect to those observed for **Ca(2)** (O4···O7 = 4.63 Å and O12···O15 = 4.66 Å, compared to O4···O7 = 3.22 Å in **Ca(2)**).

The other donor groups are distributed on both sides of the O_4 plane, resulting in a bicapped trigonal prismatic coordination for both calcium ions. The two prismatic coordination sets share the O7···O12 edge and the O17 capping donor. In the dimeric unit, the O_4 mean planes are perpendicular (diehdral angle = 86.45(5)°) and the Ca1···Ca2 distance is 3.71 Å. The Ca−O bond distances are more regular than in **Ca(2)**, even if the interaction to the oxygen bonded to the chiral carbon (O3 and O14 for Ca1 and Ca2 respectively) is still the weakest one among the O_4 donors. As regards the aromatic substituent, in both cases is roughly perpendicular to the ligand arms, while the nitro group is slightly rotated only in one case (C13−C18−N2−O10 = 39.2(4)°). The intramolecular C−H···O interactions between the chiral carbon and the nitro group are slightly weaker than in **Ca(2)** (C7−H···O1, C···O = 2.730(3) Å, H···O = 2.191(2) Å, C−H···O = 113.2(5)°; C19−H···O10, C···O = 2.883(4) Å, H···O = 2.379(3) Å, C−H···O = 111.3(1)°).

The assembly of the dimers in a covalent polymeric structure is due to the coordination of the carboxylic oxygens O5 and O16 to adjacent symmetry-related dimers lying on perpendicular planes. The resulting chain shows a stair−step undulating polymeric structure (Figure 4a−c).

The hydrogen bonds formed by the ordered water molecules are reported in Table 7.

Spectral Properties. The neutral aqueous solutions of the ligand $\mathbf{H_2L^1}$ shows the absorbance typical of *o*-nitrobenzyl compounds, with a peak located at 264.5 nm and a shoulder extending to almost 400 nm due to a $n \rightarrow \pi^*$ transition. The position of the peak at 264.5 nm is essentially unaffected by the complexation with Ca^{2+}; the spectrum is only marginally changed in the shoulder. The molar extinction coefficient for the Ca^{2+} complex at 355 nm is approximately 260 M^{-1} cm^{-1}. The ligand and the Ca^{2+} complex do not show any significant fluorescence emission when excited at 355 nm.

Table 7. List of Hydrogen Bonds in the Crystal Structure of **Ca(1)**[a]

	D···A (Å)	H···A (Å)	D−H···A (deg)
O18−H1···O13	2.608(4)	1.74(3)	160(3)
O19−H1···O8	2.998(4)	2.11(2)	173(2)
O18−H2···O8(1)	2.663(3)	1.80(2)	164(2)
O17−H1···O15(2)	2.611(2)	1.72(3)	173(2)
O17−H2···O4(3)	2.638(2)	1.77(2)	168(2)
O19−H2···O13(4)	2.675(4)	1.83(2)	156(2)

[a] Equivalent positions: (1) $x-1, y, z$; (2) $2-x, -y, 1-z$; (3) $1-x, -y, 1-z$; (4) $2-x, 1-y, 1-z$.

Photolysis was obtained by irradiation of a ligand solution with the 355 nm laser with an average power of 0.5 W until the absorbance spectrum did not show any change. The band at 264.5 nm vanishes, and a structureless broad band appears in the near UV, with a tail extending to almost 500 nm.

The addition of methoxy groups at positions 4 and 5 of the aromatic ring changes the absorbance spectrum of $\mathbf{H_2L^2}$, as expected. The peak at 264.5 nm observed for $\mathbf{H_2L^1}$ vanishes, and in $\mathbf{H_2L^2}$ new peaks at 218, 244, and 347.5 nm appear. The lower energy of the electronic transition has been attributed to the increased electronic delocalization introduced by the two methoxy groups. Analogous spectral changes were observed for other photosensitive Ca^{2+} chelators, like DM-nitrophen[8] and DMNPE,[13] and for photoactivatable caged protons as, for instance, 4-formyl-6-methoxy-3-nitrophenoxyacetic acid.[30] As for $\mathbf{H_2L^1}$, the fluorescence emission of $\mathbf{H_2L^2}$ is negligible. The photoproducts show a structureless absorption spectrum which extends to 600 nm.

Stability of the Complexes and Calcium Release by Flash Photolysis. The dissociation constants for **Ca(1)** and **Ca(2)** have been determined by using a spectroscopic method based on the fluorescent Ca^{2+} indicator OG5N, in addition to the potentiometric method illustrated in the previous section. The low-affinity indicator OG5N is used to monitor the concentration of free Ca^{2+} in solution as a function of total **Ca(1)** or **Ca(2)** concentration. Upon increase of the concentration of the calcium complex in solution, an increase in the fluorescence emission of the indicator is observed. Free Ca^{2+} concentrations can be calculated from the fluorescence emission intensity (F, $\lambda = 525$ nm) at all calcium complex concentrations using the calibrating fluorescence intensities at saturating Ca^{2+} (F_{max}) and in the absence of Ca^{2+} (F_{min}):

$$[Ca^{2+}] = K_d^I \frac{F - F_{min}}{F_{max} - F}$$

Here K_d^I is the dissociation constant for the Ca^{2+} indicator.

In the case of **Ca(2)**, for example, the Ca^{2+} concentration increase can be modeled with the expression

(30) Janko, K.; Reichert, J. *Biochim. Biophys. Acta* **1987**, *905*, 409−416.

$$[Ca^{2+}]_{free} = [Ca^{2+}]^0 + \frac{-K_d + \sqrt{K_d^2 + 4K_d[\mathbf{Ca(2)}]}}{2}$$

where [**Ca(2)**] is the total concentration of **Ca(2)**, K_d is the dissociation constant of **Ca(2)**, and $[Ca^{2+}]^0$ is the concentration of free Ca^{2+} before to the addition of the complex. Fitting of the data gave the value $K_d = 2.1 \pm 0.1$ μM. Very similar data were obtained for **Ca(1)**, for which the dissociation constant resulted $K_d = 2.6 \pm 0.2$ μM. These values agree with the one obtained by using potentiometric measurement, on considering the effect of the different solvents (see previous section).

The stability of **Ca(1)** and **Ca(2)** was tested by the addition of increasing amounts of NaCl, KCl, and $MgCl_2$. As usual, the level of free Ca^{2+} was monitored by the fluorescence emission of the Ca^{2+} indicator OG5N. In Figure 5, the (a) curve represents the fluorescence emission of the indicator in a 1.38 mM solution of **Ca(1)** at pH = 7, while the (b) curve refers to the fluorescence emission of the same solution ([NaCl] = 0.16 M). The fluorescence intensity is essentially unaffected, indicating that the level of free Ca^{2+} did not change on addition of NaCl. Similar results were found by using KCl and $MgCl_2$ instead of NaCl. No calcium release was observed up to a molar ratio of 1:100 Ca^{2+}/competitive ion for both the complexes. These results are in accord with the stability constants found by potentiometric methods for the Mg^{2+} and Ca^{2+} complexes and indicate a higher selectivity of both the ligands for calcium over magnesium (ca. 2.5×10^2 fold; see previous section).

Effectively, photolysis of **Ca(1)** and **Ca(2)** efficiently leads to the release of Ca^{2+} into the solution. Figure 6shows the effect of the photolysis of **Ca(1)** with a frequency tripled Nd:YAG laser (355 nm, 1 W on the sample): the absorbance of OG5N increases in response to the Ca^{2+} released by the photolyzed **Ca(1)**. Binding of the indicator occurs with an apparent lifetime of 9.6 μs and relaxation to equilibrium can be described with an apparent lifetime of 230 μs. Similar results were obtained with **Ca(2)**.

Conclusions

The $\mathbf{H_2L^1}$ and $\mathbf{H_2L^2}$ ligands react with calcium ions to give the **Ca(1)** and **Ca(2)** complexes. In the solid state, they are formed by dimeric units with the carboxylic groups bridging the metal ions; calcium ions result as octacoordinate. The reduction of the 2-nitrobenzyl chromophore by photolysis causes the rupture of the ligand and the consequent release in solution of the calcium ions; the transient changes in free Ca^{2+} concentration were studied by flash photolysis.

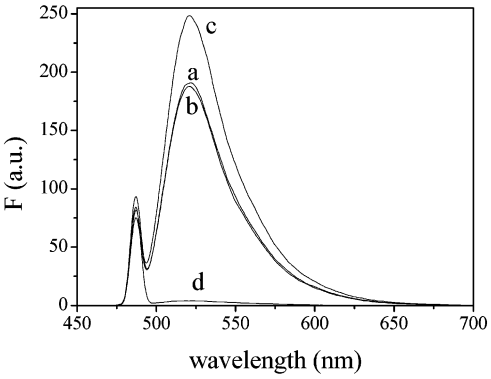

Figure 5. Fluorescence emission of the Ca^{2+} indicator OG5N (2 μM) in a 1.38 mM solution of **Ca(1)**. The curves refer to the following conditions: (a) [NaCl] = 0 M; (b) [NaCl] = 0.16 M; (c) $[Ca^{2+}]$ = 0.02 M. This concentration corresponds to the saturation of the indicator; (d) $[Ca^{2+}]$ = 0 M.

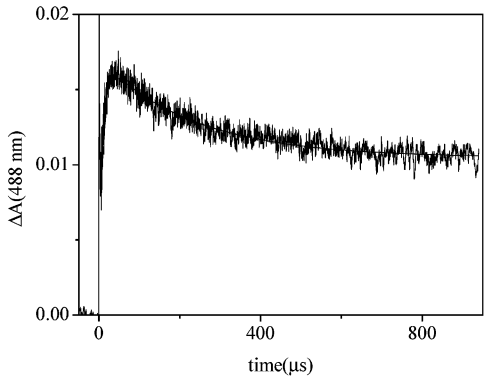

Figure 6. Transient changes in free Ca^{2+} concentration in a **Ca(1)** solution as monitored at 488 nm by the transient absorption of OG5N, following a single laser pulse.

The possibility to obtain UV-triggered Ca^{2+} jumps and the good stability in the presence of competitive ions make **Ca(1)** and **Ca(2)** interesting tools for biochemical studies. Effectively, a first application has been already carried out: they were used to study the mechanism of calcium extrusion in hair cells mechanically isolated from frog semicircular canals.[31]

Acknowledgment. The authors acknowledge financial support from INFM (Istituto Nazionale per la Fisica della Materia, PRA CADY and PAIS UNCAGE2 projects).

Supporting Information Available: UV absorbance spectra and crystallographic data in CIF format. This material can be obtained free of charge via the Internet at http//pubs.acs.org.

IC034059T

(31) Martini, M.; Rossi, M. L.; Farinelli, F.; Moriondo, A.; Mammano, F.; Rispoli, G. *Eur. J. Neurosci.* **2002**, *16*, 1647−1653.